JAEA-Technology
2013-010

Fuel Temperature Analyses of Metallic Fuel Pins for Sodium-cooled Fast Reactors

Tomoyasu MIZUNO, Shin-ichi KOYAMA, Takeji KAITO
Tomoyuki UWABA and Kenya TANAKA

Fast Reactor Fuels and Materials Technology Development Unit
Advanced Nuclear System Research and Development Directorate

June 2013

Japan Atomic Energy Agency

日本原子力研究開発機構

JAEA-Technology

本レポートは独立行政法人日本原子力研究開発機構が不定期に発行する成果報告書です。
本レポートの入手並びに著作権利用に関するお問い合わせは、下記あてにお問い合わせ下さい。
なお、本レポートの全文は日本原子力研究開発機構ホームページ（http://www.jaea.go.jp）
より発信されています。

独立行政法人日本原子力研究開発機構　研究技術情報部　研究技術情報課
〒319-1195　茨城県那珂郡東海村白方白根 2 番地 4
電話 029-282-6387, Fax 029-282-5920, E-mail:ird-support@jaea.go.jp

This report is issued irregularly by Japan Atomic Energy Agency
Inquiries about availability and/or copyright of this report should be addressed to
Intellectual Resources Section, Intellectual Resources Department,
Japan Atomic Energy Agency
2-4 Shirakata Shirane, Tokai-mura, Naka-gun, Ibaraki-ken 319-1195 Japan
Tel +81-29-282-6387, Fax +81-29-282-5920, E-mail:ird-support@jaea.go.jp

JAEA- Technology 2013-010

Fuel Temperature Analyses of Metallic Fuel Pins for Sodium-cooled Fast Reactors

Tomoyasu MIZUNO, Shin-ichi KOYAMA, Takeji KAITO, Tomoyuki UWABA and Kenya TANAKA

Fast Reactor Fuels and Materials Technology Development Unit,
Advanced Nuclear System Research and Development Directorate,
Japan Atomic Energy Agency
Oarai-machi, Higashiibaraki-gun, Ibaraki-ken

(Received March 11, 2013)

Metallic fuel, U-Pu(TRU)-Zr, is a fuel candidate for Sodium-cooled fast reactor (SFR) selected as a possible promising future nuclear reactor system in Generation-IV international forum (GIF). Design studies were performed in the Japanese feasibility study on commercialized fast reactor cycle system, and the irradiation behavior of metallic fuel is under investigation through analytical fuel performance code calculations with preliminary analytical models. Some calculations of U-Pu(TRU)-Zr fuel irradiation performance were conducted by a simplified calculation grogram developed in JAEA. The fuel temperatures during irradiation with two kinds of effective fuel thermal conductivity, with and without sodium ingress into the fuel slug were calculated.

Calculated fuel temperature during steady state operation of the core was low enough to avoid fuel melting even with the former effective fuel thermal conductivity which gives higher temperature conservative enough for reactor license application. In case of the latter effective fuel thermal conductivity, the fuel temperature had more margin to the fuel melting. Axial profile of fuel pin centerline temperature in case of the latter effective fuel thermal conductivity revealed that its peak axial position is over X/L=0.7, whereas it is below X/L=0.7 in case of the former effective fuel thermal conductivity. Based on the irradiation test results, the axial temperature profile of the latter effective fuel thermal conductivity fits well with actual fuel micro structures after the irradiation. The effective fuel thermal conductivity with sodium ingress is suitable for the irradiation behavior investigation.

Keywords：Fast Reactor, Metallic Fuel, Fuel Temperature, Calculation Code

JAEA- Technology 2013-010

ナトリウム冷却高速炉のための金属燃料ピンの燃料温度解析

日本原子力研究開発機構　次世代原子力システム研究開発部門
燃料材料技術開発ユニット

水野　朋保、小山　真一、皆藤　威二、上羽　智之、田中　健哉

(2013 年 3 月 11 日　受理)

U-Pu(TRU)-Zr,を成分とする金属燃料は、第 4 世代原子力国際フォーラム (GIF)において、有望な原子炉として選定されたナトリウム冷却炉(SFR)の候補燃料の一つである。金属燃料の設計研究は日本における高速増殖炉サイクルの実用化戦略調査研究で実施され、照射挙動に関して、挙動解析コードを用いた予備評価を実施中である。JAEA において、U-Pu(TRU)-Zr 燃料の照射挙動評価を簡易計算プログラムにより実施した。この評価では、燃料スラグ中へのナトリウムの侵入の有無を考慮し、２種類の実効燃料熱伝導度を用いた。

定常運転時の燃料温度は非常に低く、許認可性を考慮するため高めの温度を計算するように燃料スラグへのナトリウム侵入がない保守的な熱伝導度モデルを用いた場合でさえも、燃料温度は融点を下回る評価結果となった。ナトリウム侵入を考慮する場合は、燃料温度は溶融に対して更に余裕のある評価結果となった。燃料へのナトリウム侵入を考慮する場合、燃料温度が最高となる軸位置は X/L=0.7 より上部となるが、ナトリウム侵入を考慮しない場合には、これよりも下部側となった。ナトリウム侵入を考慮した実効熱伝導度による燃料軸方向温度分布は、照射後の実際の燃料組織と良く整合する結果となった。これより、ナトリウム侵入を考慮した燃料実効熱伝導は、照射挙動評価に適すると考えられる。

大洗研究開発センター（駐在）：〒311-1393　茨城県東茨城郡大洗町成田町 4002

Contents

目　次

List of table

List of figure

This is a blank page.

1. Introduction

Sodium-cooled fast reactors (SFR) were selected in Generation-IV international forum (GIF) as a possible promising future nuclear reactor system with superior safety, sustainability and economic competitiveness.[1] Fuel candidates for SFR in GIF collaborative program include U-Pu(TRU)-Zr metallic fuel as well as oxide fuel.[2]

Design studies of metallic fuel core for SFR were performed in the Japanese feasibility study on commercialized fast reactor cycle systems. The significant outcome of the studies is an attractive core and fuel concept which achieves high burnup and high outlet temperature of reactor vessel.[3] The irradiation behavior of metallic fuel of the design studies is under investigation through analytical fuel performance code calculations with preliminary analytical models of metallic fuel.

In the present work, analytical code calculations of metallic fuel pin irradiation performance are conducted with major interest on fuel temperatures during irradiation.

The irradiation behavior models and fuel properties for the analytical code were selected based on the information of metallic fuel characteristics including fuel properties and irradiation behavior obtained from open literatures and collaborative research activities with the Central Research Institute of Electric Power Industry.

2. Outline of calculation program

A simplified calculation program for U-Pu(TRU)-Zr metallic fuel pin performance analysis has been developed. This program is an R-Z system and models the thermal behaviors of a fuel pin during irradiation using 10 axial nodes, each having 26 radial nodes, 20 of which are for the fuel region and 6 for the cladding region. Mass transports in the direction are not taken into account, except for FP gases released into the gas plenum of the fuel pin. The program is limited to analyses of fuel pins having a smear density not over around 75%TD. Table 1 shows the evaluated behaviors. Some conservative and simplified models as follows were incorporated into the program;

1) for the FP gas release, the fractional release rate under irradiation was taken as the constant value of 90 %,

2) for the fuel and cladding mechanical analyses, the fuel-cladding contact pressure under irradiation was taken as the constant value of zero, because it was reported that no considerable contacts between fuel and cladding were obtained in the case of fuels having a smear density of less or equal to 75%TD.[4] Only the stress-strain analysis of cladding due to the plenum gas pressure were conducted,

3) for the fuel restructuring and fuel constituents migrations, they were not taken into account,

4) for the fuel thermal conductivity, metallic fuel slug effective thermal conductivity is considered. The effective thermal conductivity model consists of solid fuel slug thermal conductivity with 100% TD and contribution of porous fuel microstructure filled with gas and liquid sodium due to gas swelling and sodium ingress under irradiation. The correlations of solid fuel thermal conductivity and contribution of porous fuel

microstructure are found elsewhere.[5-7] The volume fractions of gas-filled porosity and sodium-infiltrated porosity are treated as variants in the present work. The specific conditions in the calculation are described later.

The finite difference analysis procedure is applied to the thermal analysis, and the stress-strain analysis procedure based on the generalized plane strain is applied to the mechanical analysis of cladding. Figures 1 and 2 show the geometrical model and flow chart of the program, respectively.

3. Calculation conditions

3.1 Fuel pin specifications and irradiation conditions

Table 2 shows fuel specifications and irradiation conditions for this investigation. A fuel pin having a metallic U-Pu-Zr slug with the ODS cladding was taken for this investigation. The bonding material filling the fuel-cladding gap was sodium. The level of bonding sodium was up to the top of the fuel column. The irradiation time was taken as 2205 days (3 cycles). The maximum neutron fluence was taken as 5.50×10^{23}n･cm^{-2}, then the maximum local burnup was evaluated to be as 140 GWd/t. The coolant inlet temperature was taken as 668K. Calculations were conducted at the following 5 axial positions; X/L = 0.9, 0.7, 0.5, 0.3, and 0.1. Axial distribution conditions at BOL and EOL of LHR and cladding midwall temperature are shown in Figs. 3 and 4, respectively. Profile conditions of LHR and cladding midwall temperature at each axial position of the calculations are shown in Figs. 5 and 6, respectively.

These conditions are based on the current results of feasibility studies on a commercialized fast reactor cycle system in Japan.[3]

3.2 Effective thermal conductivity models of metallic fuel

As described above, the effective thermal conductivity model consists of solid fuel slug thermal conductivity with 100% TD and contribution of porous fuel microstructure filled with gas and liquid sodium. The fraction of swelled volume filled with sodium was reported to be from 0.25 to 0.28 in some case of U-Pu-Zr fuel. In the present study, following two cases are selected aiming at a sensitivity study. One is 0.25 of the fraction as a case of sodium ingress and the other is no sodium ingress as conservative case.

4. Results and discussions

From Fig. 7 to Fig. 11, the evaluated fuel temperature histories using the effective thermal conductivity with sodium ingress are shown. It is easily seen that fuel temperature increased with burnup in the early stage of each cycle and slightly decreased with burnup in the later stage of each cycle. The evaluated gap width between fuel and cladding at each axial position are shown in Fig.12. It is easily seen that the gap between fuel and cladding closed in the early stage of the irradiation. After that, the gap conductance was so high that it had little contribution to the fuel temperature. Then, the obtained temperature profiles were

attributed to the profile conditions of LHR.

Figures 13 and 14 show the evaluated fuel temperature histories of X/L=0.5 and 0.7 using the effective thermal conductivity without sodium ingress. The fuel temperatures are high in comparison with those in Figs. 8 and 9 due to the low effective thermal conductivity.

Figures 15 through 18 show the radial temperature distributions of both thermal conductivities at EOL of X/L=0.5 and 0.7. In case of the effective thermal conductivity without sodium ingress, temperature gradient in the fuel surface becomes steep due to the low thermal conductivity.

Figure 19 shows the evaluated history of pressure on the cladding inner surface due to the plenum gases. Figure 20 shows the evaluated cladding deformation after the irradiation. The results show that the fuel pin had enough plenum volume not to cause considerable cladding deformations by plenum gas pressure.

Therefore, it is concluded that the metallic U-Pu-Zr fuel pin having the specifications and irradiation conditions used in this investigation would be irradiated moderately up to approximately 140GWd/t with well integrity.

Figures 21 and 22 show the fuel centerline temperatures of 0.4%Am(in heavy metal) bearing fuel with the effective thermal conductivity with sodium ingress at X/L=0.5 and 0.7. In this calculation Am contribution was assumed to be same as it of Pu. Therefore, fuel thermal conductivity slightly decreases and fuel centerline temperature of Am bearing fuels slightly higher than that of U-Pu-Zr fuel, as shown in these figures. The difference of these temperatures is limited within one degree C. The contribution of Am inclusion may not be significant when the Am content is less than 1% of heavy metal.

Figures 23 and 24 show axial distributions of fuel centerline temperature. The fuel centerline temperatures of thermal conductivity without sodium ingress are more conservative than those with sodium ingress by about 100 degree C. In viewpoint of axial position of fuel maximum temperature, it is over X/L=0.7 in case of the thermal conductivity with sodium ingress, whereas it is between X/L=0.5 and 0.7 in case of the thermal conductivity without sodium ingress. In irradiation tests of metallic fuel, the fuel micro structures observed in post irradiation examinations tell that axial position of maximum fuel centerline temperature must be close to the top region of fuel column rather than the axial center region. In this view, the case of thermal conductivity with sodium ingress may be more realistic as far as the axial distribution of fuel temperature is concerned.

5. Conclusion

Some calculations of metallic fuel irradiation performance were conducted by a simplified calculation program developed in JAEA to understand the behavior of a U-Pu(TRU)-Zr fuel pin. The major interest of the investigation is calculated fuel temperatures during irradiation with two kinds of effective fuel thermal conductivity, with and without sodium ingress into the fuel slug.

Calculated fuel temperature during steady state operation of the core was low enough to avoid fuel melting even with the former effective fuel thermal conductivity which gives higher temperature conservative enough for reactor license application. In case of the latter effective fuel thermal

conductivity, the fuel temperature had more margin to the fuel melting. Axial profile of fuel pin centerline temperature in case of the latter effective fuel thermal conductivity revealed that its peak axial position is over X/L=0.7, whereas it is below X/L=0.7 in case of the former effective fuel thermal conductivity. Based on the irradiation test results, the axial temperature profile of the latter effective fuel thermal conductivity fits well with actual fuel micro structures after the irradiation. The effective fuel thermal conductivity with sodium ingress is suitable for the irradiation behavior investigation.

In case of 0.4%Am bearing fuel, calculation result shows that fuel centerline temperature becomes high, but increase from U-Pu-Zr fuel is insignificant.

Other characteristics of fuel irradiation performance such as fuel pin internal gas pressure history and cladding deformation show that the fuel pin keeps its integrity through its irradiation duration.

References

1) Y. Sagayama, "Feasibility Study on Commercialized Fast Reactor Cycle Systems (1) Current Status of the Phase-II Study", Global 2005, No.380, Tsukuba, Japan (2005).
2) S. Kotake, et al., "Feasibility Study on Commercialized Fast Reactor Cycle Systems / Current Status of the FR System Design", Global 2005, No.435, Tsukuba, Japan (2005).
3) K.Sugino et al., "Advanced Metal Fuel Core Design Study for SFR in the "Feasibility Study" in Japan", Global 2005, No.399, Tsukuba, Japan (2005).
4) G. L. Hofman, R. G. Pahl, C.E. Lahm, and D. L. Porter, "Swelling behavior of U-Pu-Zr fuel", Metallurgical Trans. A, vol. 21A, p.517(1990).
5) T.Ogata, J.Nucl. Scie. Technl., Supplement 3, pp.675-681 (2002).
6) T.H.Bauer and J.W.Holland, "in-pile Measurement of the Thermal Conductivity of Irradiated Metallic Fuel", J.Nucl. Technl., Vol.110, pp.407-421 (1995).
7) T.H.Bauer, "A General Analytical Approach toward the Thermal Conductivity of Porous Media", Int. J. Heat Mass transfer, Vol.36, p.4181 (1993).

Table 1 Behaviors evaluated by the calculation program

Evaluated fuel behaviors
Temperature distribution Thermal expansion Fission gas release Swelling
Evaluated cladding behaviors
Temperature distribution Thermal expansion Void swelling Creep deformation due to plenum gas pressure Cladding corrosion due to FPs Cladding liquid phase penetration Creep damage

Table 2 Designed fuel specifications and irradiation conditions

Item		Unit	Value
Fuel	Type		Slug
	Outer diameter	mm	6.496
	Density	%TD	100
	Pu cont.(including MA)	wt.%	11.47
	Zr cont.	wt.%	6.0
Fuel colum length		mm	750
Plenum	upper	mm	1350
Cladding	Material		ODS
	Inner diameter	mm	7.5
	Outer diameter	mm	8.5
	Thickness	mm	0.5
Bonding	Material		Sodium
	Filling level	mm	up to fuel column
Irradiation duration		day	2205 (1cycle : 735)
Max. LHR		W/cm	347
Max. Cladding midwall temperature		K	878
Max. Neutron fluence(>0.1MeV)		n/cm^2	5.50E23
Max. Burnup (local position)		GWD/t	140
Coolant	Material		Sodium
	Inlet temperature	K	668

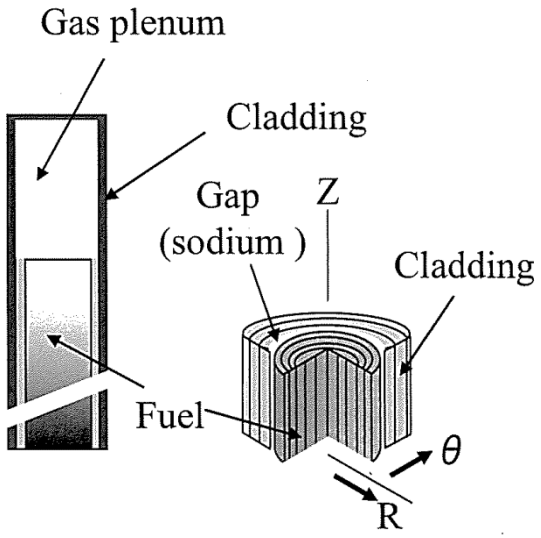

Fig.1 Geometrical model of the calculation program

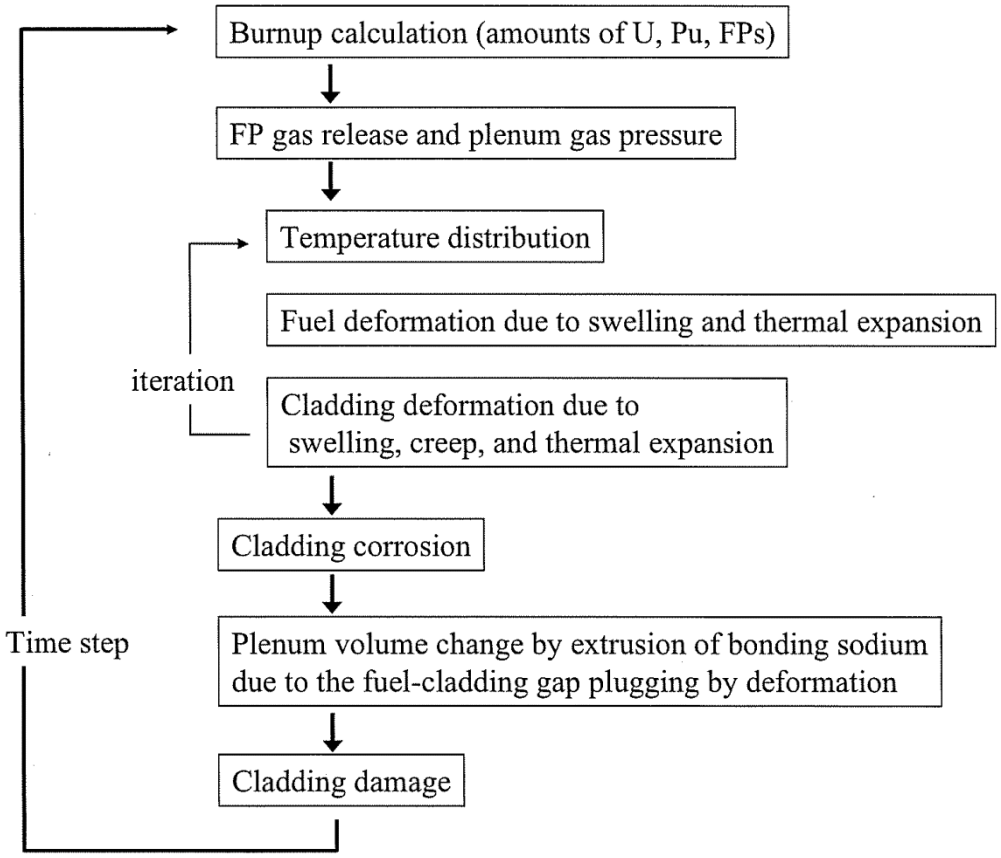

Fig.2 Flow chart of the calculation program

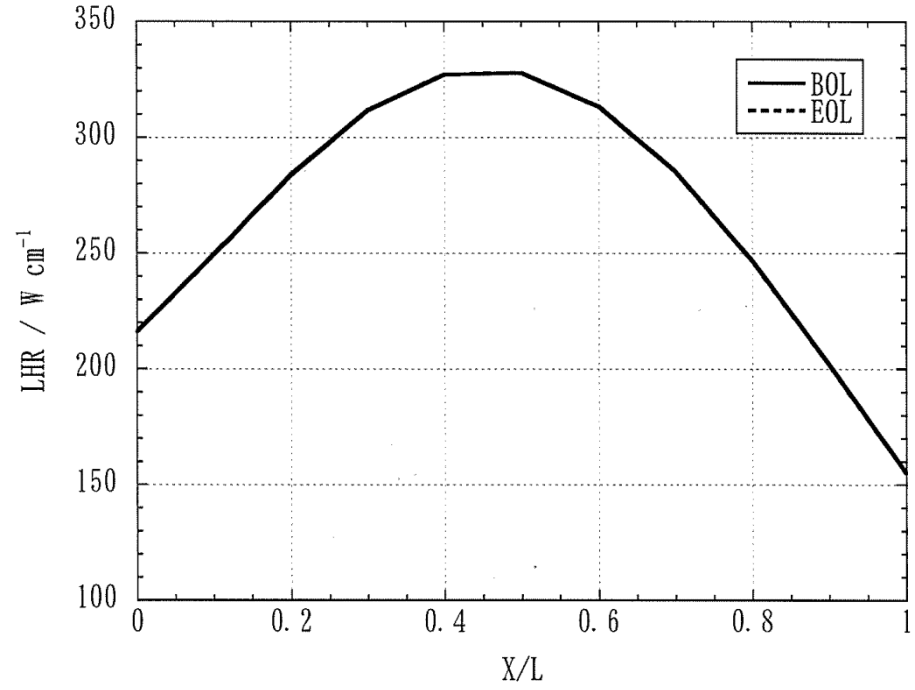

Fig.3 Axial distribution condition of LHR

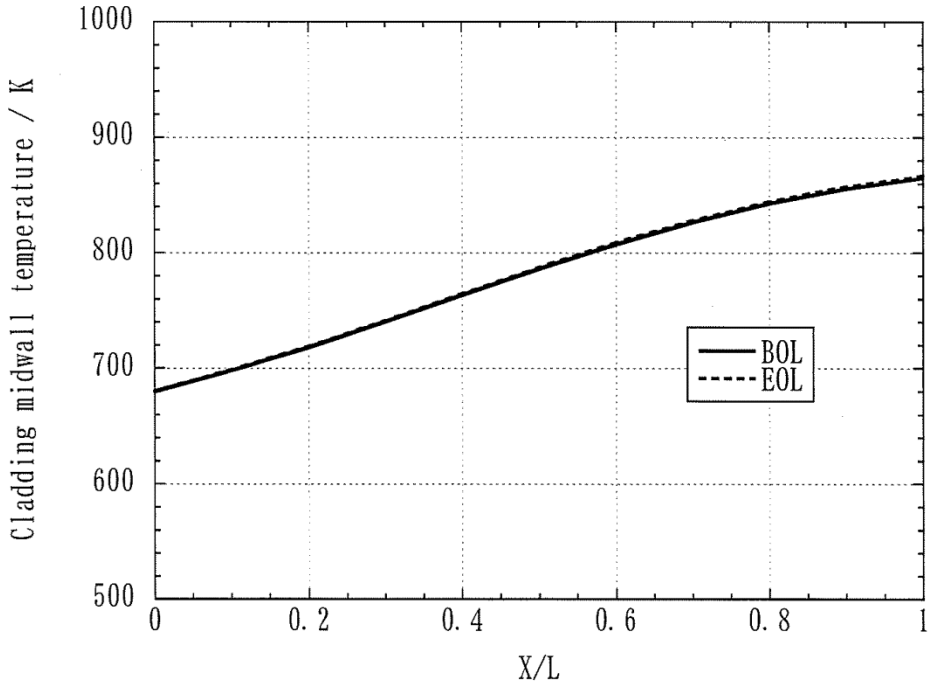

Fig.4 Axial distribution condition of cladding midwall temperature

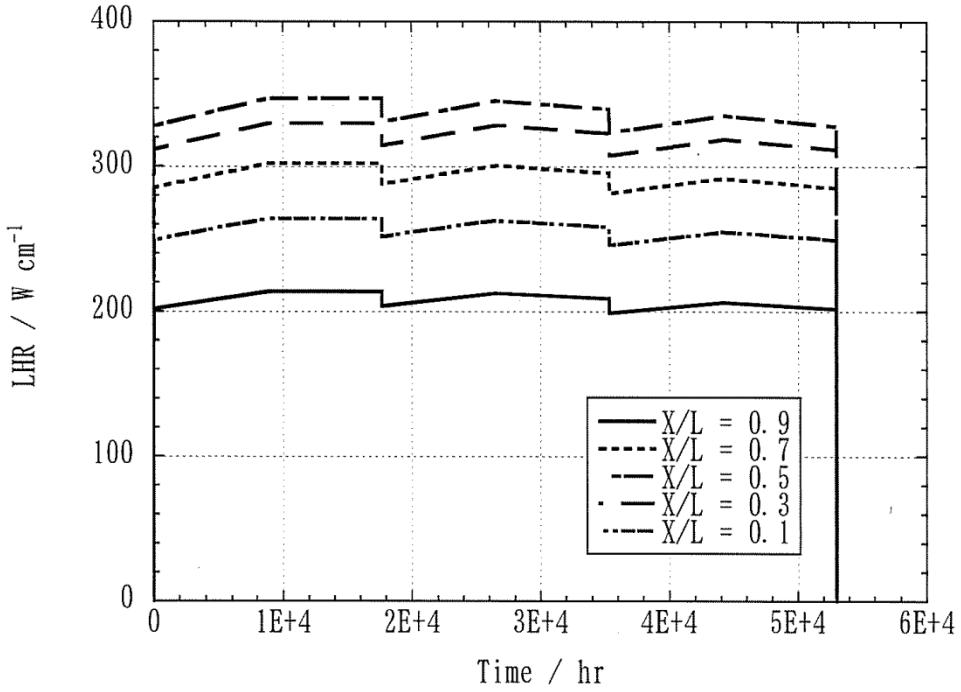

Fig.5 Profile condition of LHR

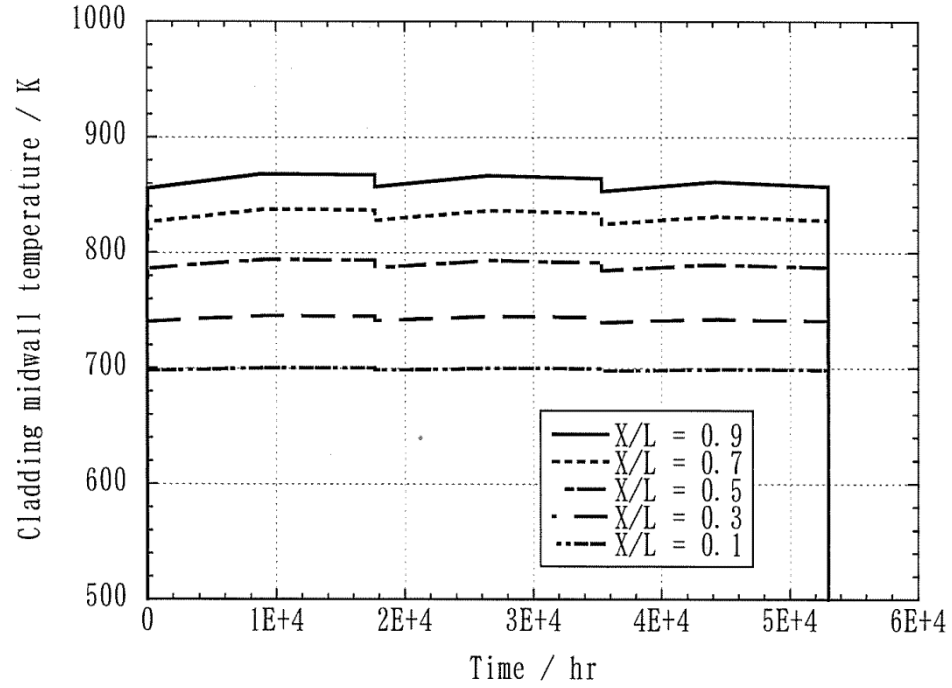

Fig.6 Profile condition of cladding midwall temperature

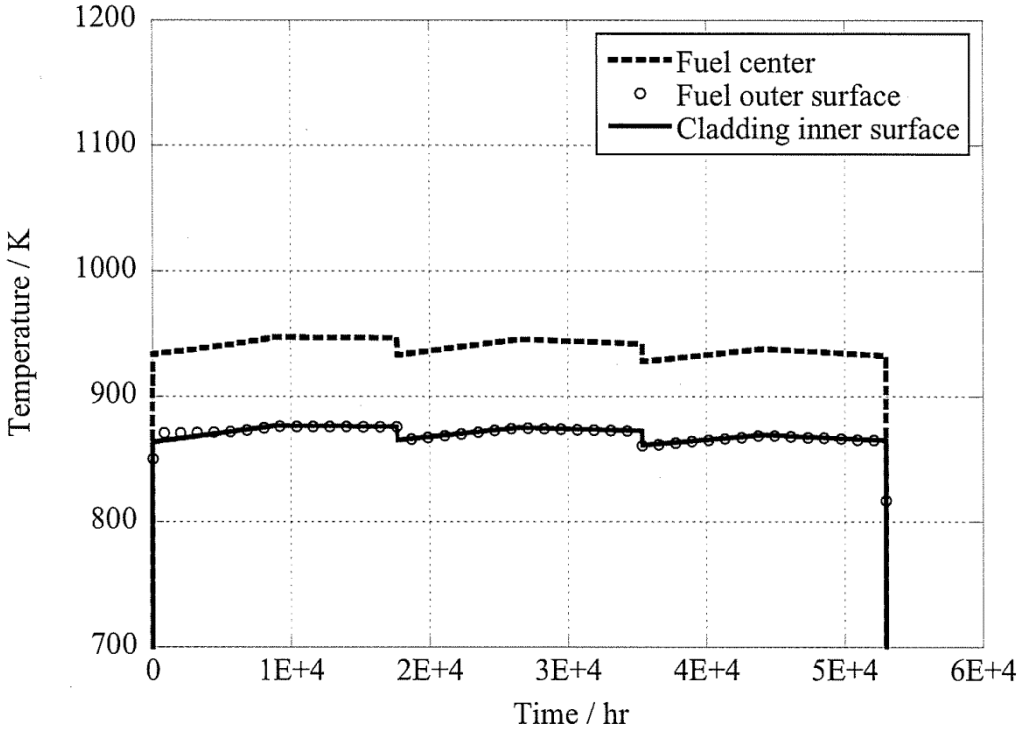

Fig.7 Temperature profiles at X/L=0.9
(Effective thermal conductivity model with sodium ingress into the fuel)

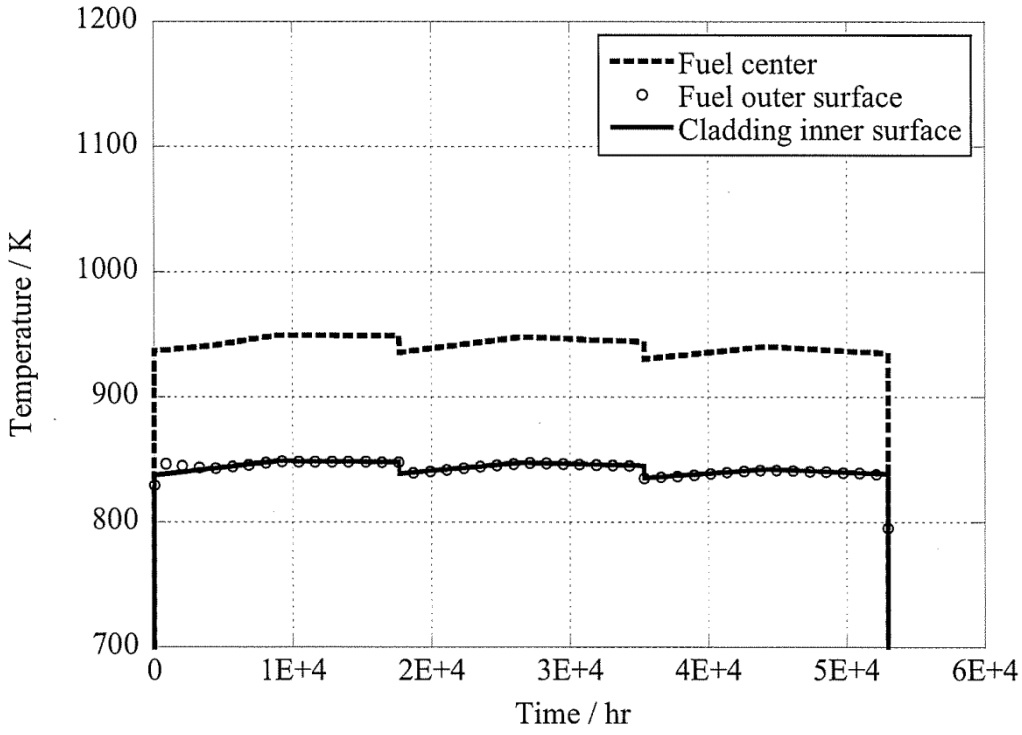

Fig.8 Temperature profiles at X/L=0.7
(Effective thermal conductivity model with sodium ingress into the fuel)

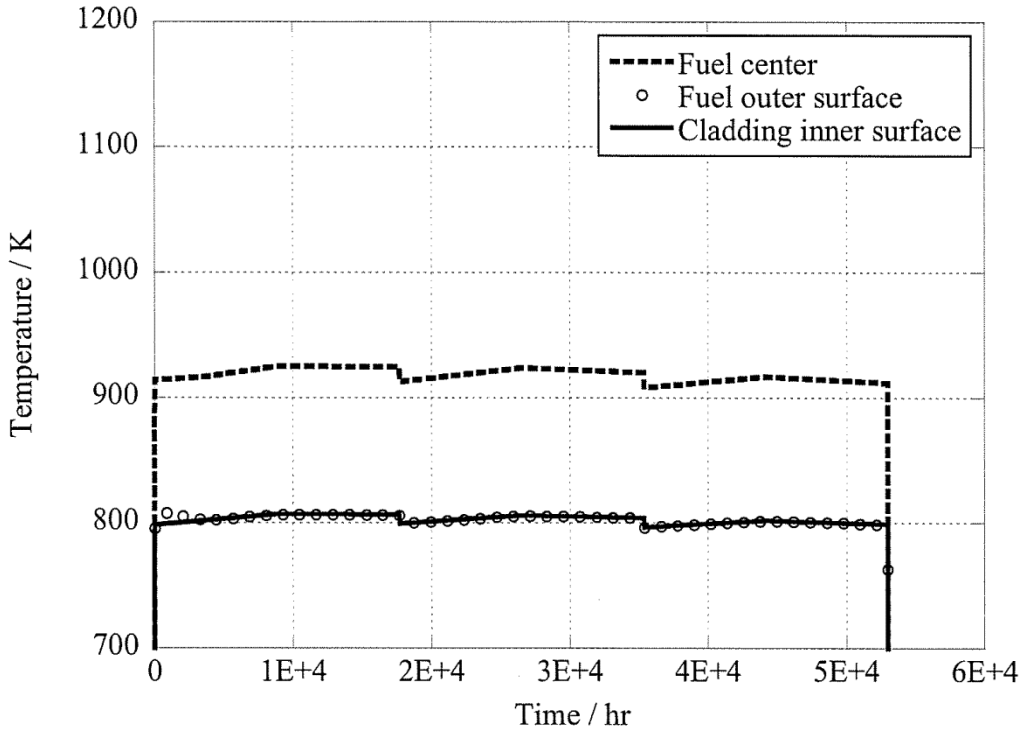

Fig.9 Temperature profiles at X/L=0.5
(Effective thermal conductivity model with sodium ingress into the fuel)

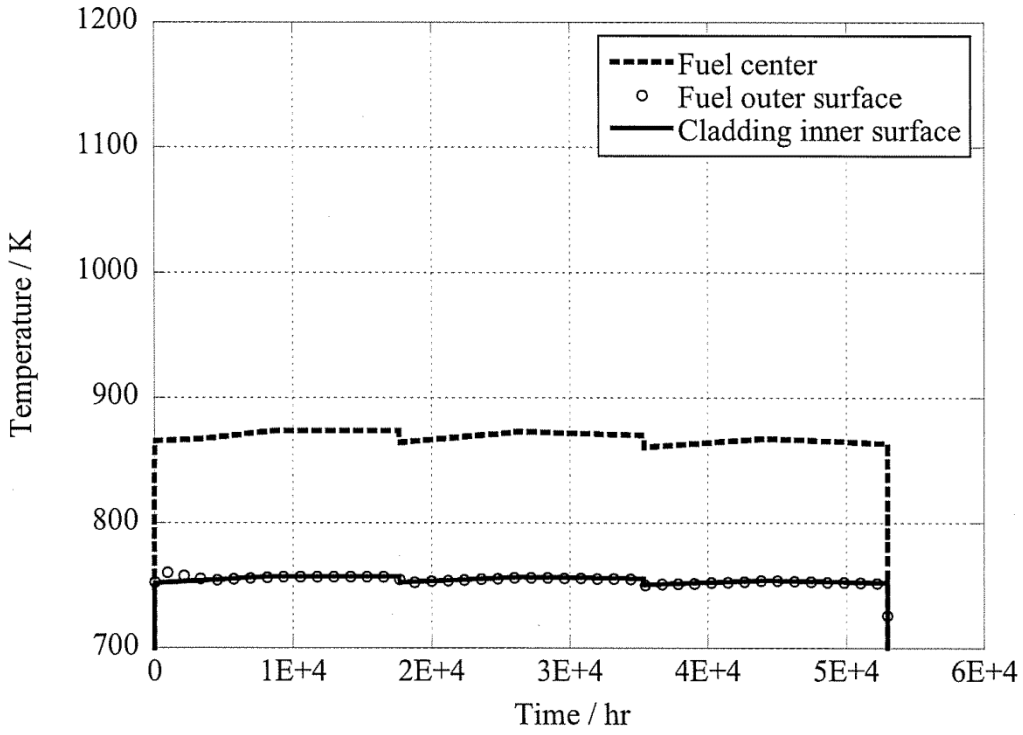

Fig.10 Temperature profiles at X/L=0.3
(Effective thermal conductivity model with sodium ingress into the fuel)

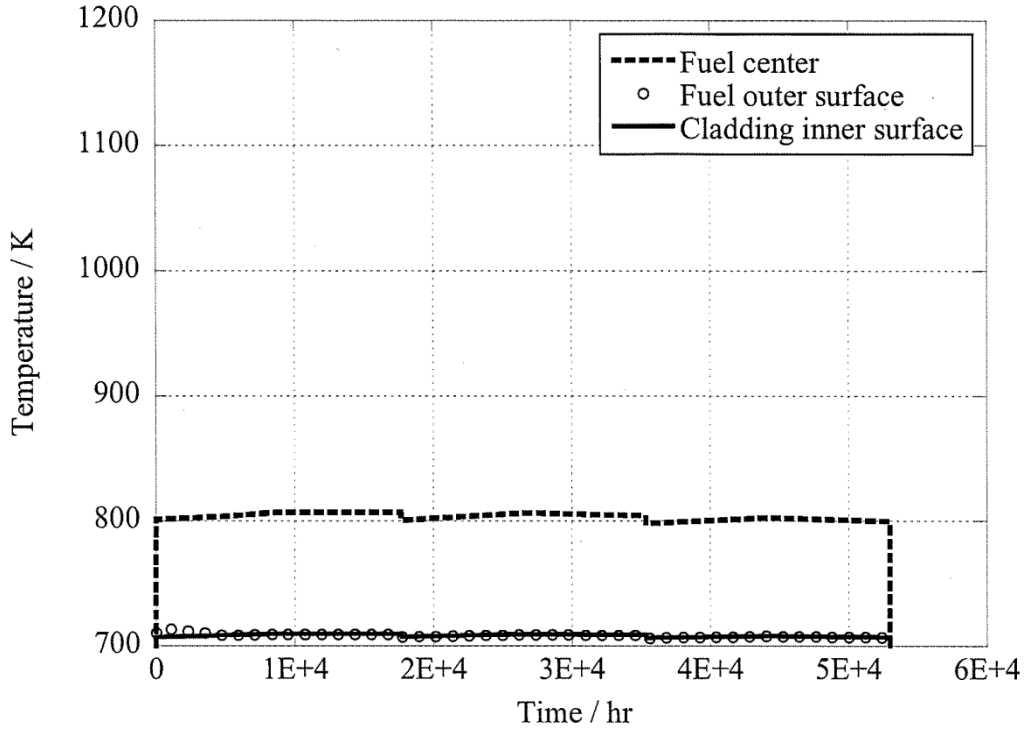

Fig.11 Temperature profiles at X/L=0.1
(Effective thermal conductivity model with sodium ingress into the fuel)

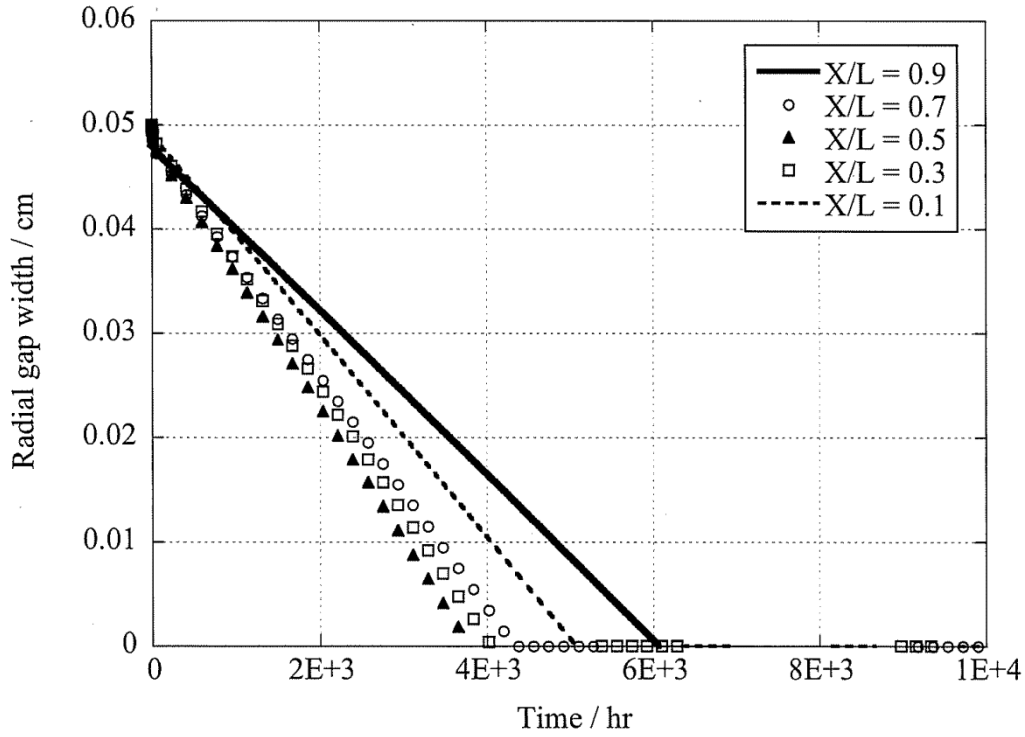

Fig.12 Profiles of gap width up to 1×10^4 hour
(From 1E4 hr to the end of irradiation, the gap was found to be plugged at each axial position.)

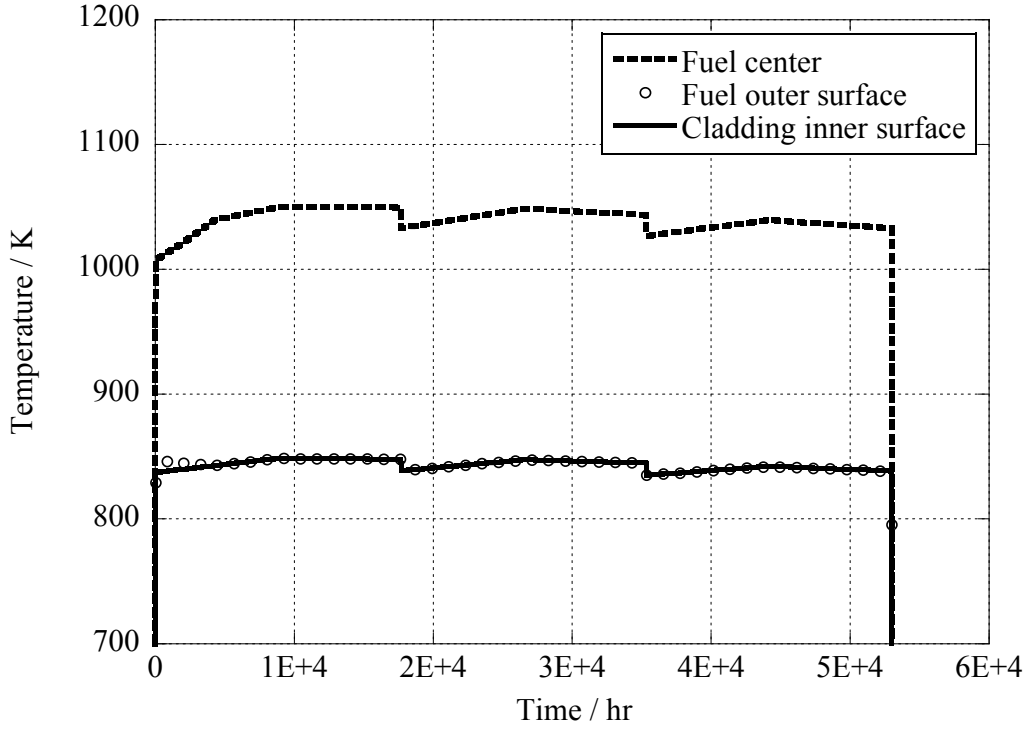

Fig.13 Temperature profiles at X/L=0.7
(Effective thermal conductivity model without sodium ingress into the fuel)

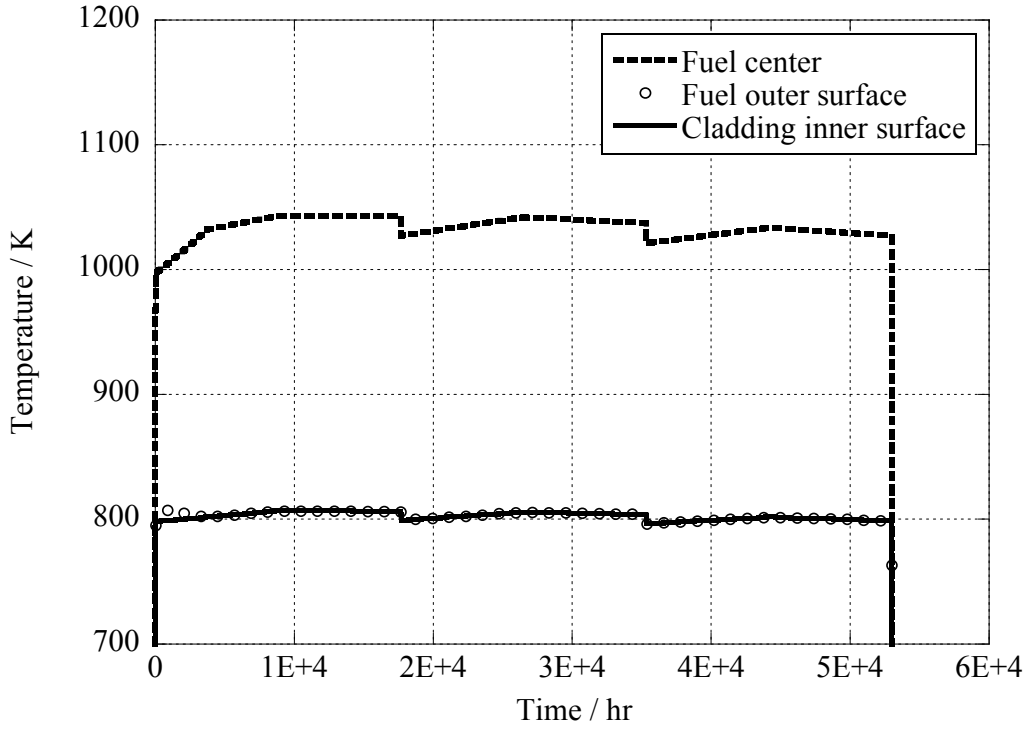

Fig.14 Temperature profiles at X/L=0.5
(Effective thermal conductivity model without sodium ingress into the fuel)

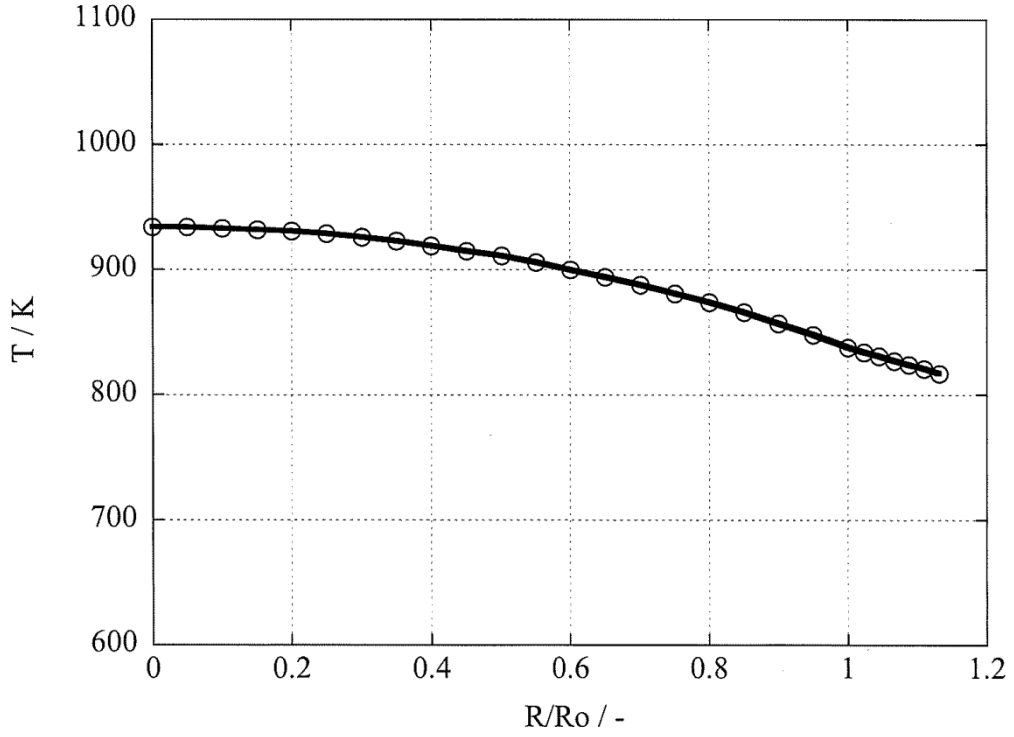

Fig.15 Radial distribution of fuel temperature at X/L=0.7
(Effective thermal conductivity model with sodium ingress into the fuel)

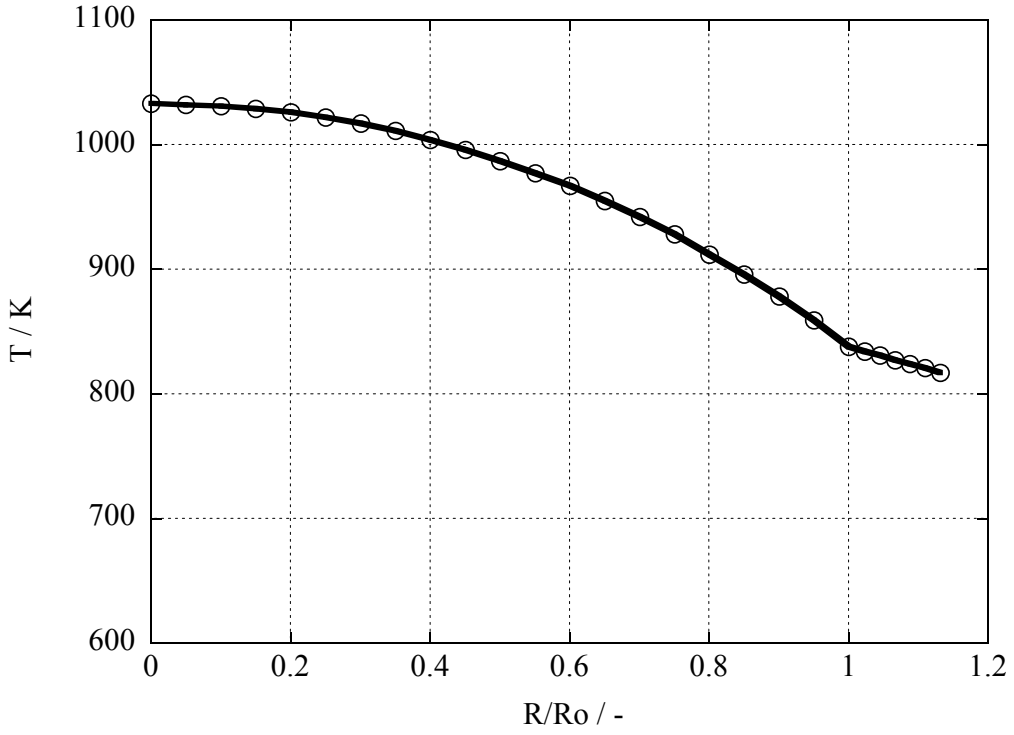

Fig.16 Radial distribution of fuel temperature at X/L=0.7
(Effective thermal conductivity model without sodium ingress into the fuel)

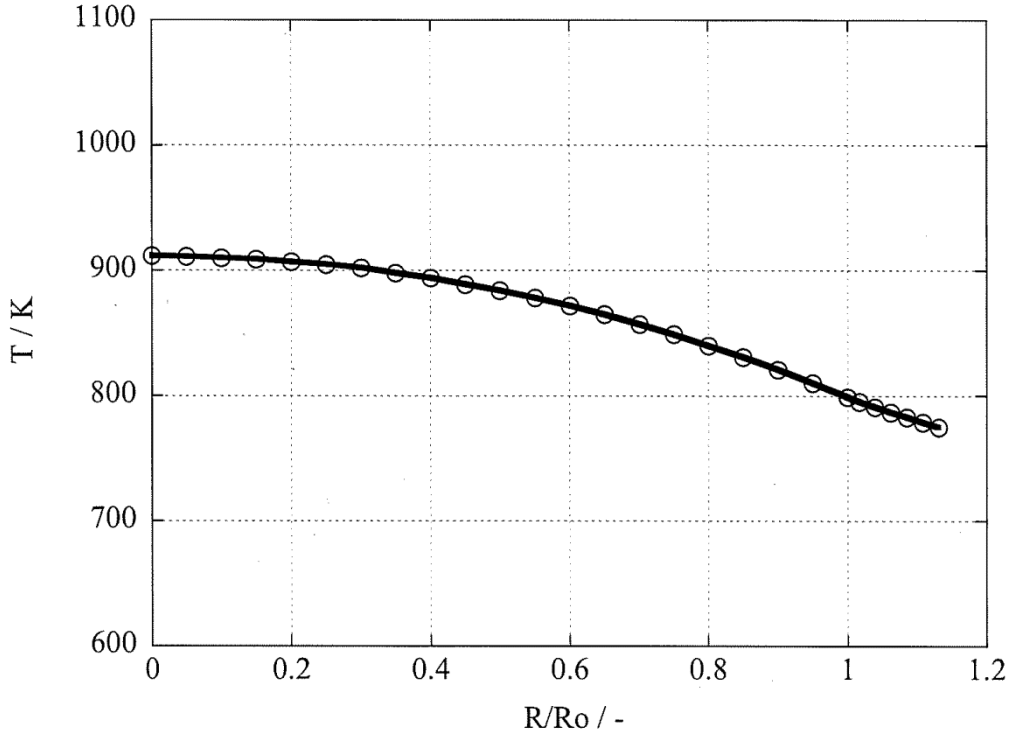

Fig.17 Radial distribution of fuel temperature at X/L=0.5
(Effective thermal conductivity model with sodium ingress into the fuel)

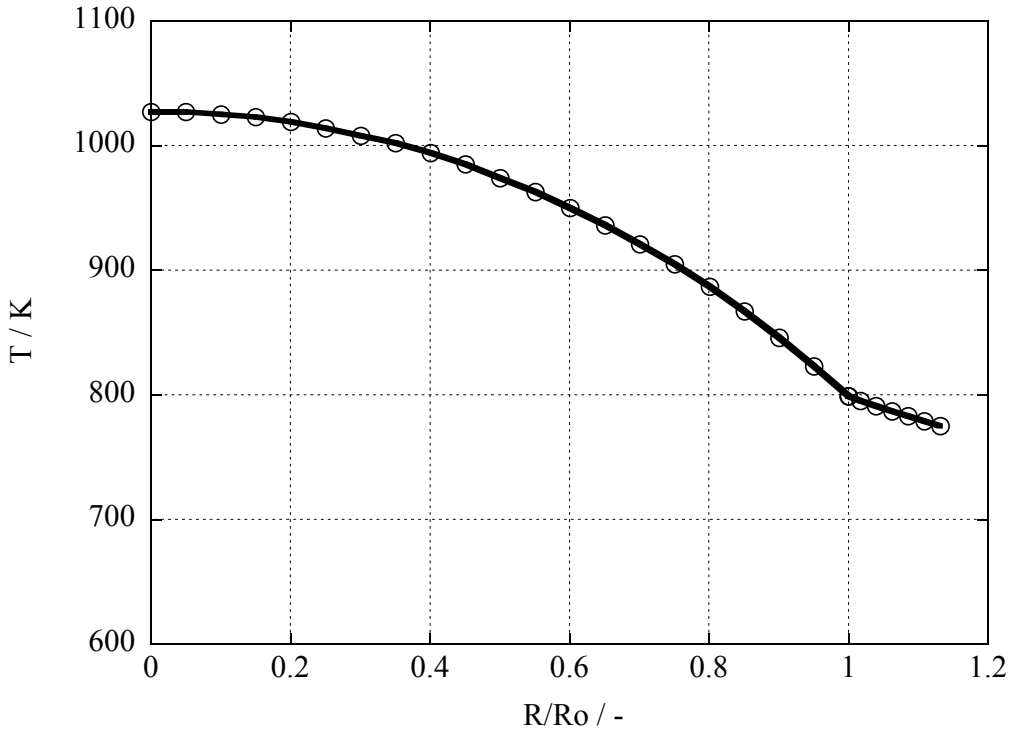

Fig.18 Radial distribution of fuel temperature at X/L=0.5
(Effective thermal conductivity model without sodium ingress into the fuel)

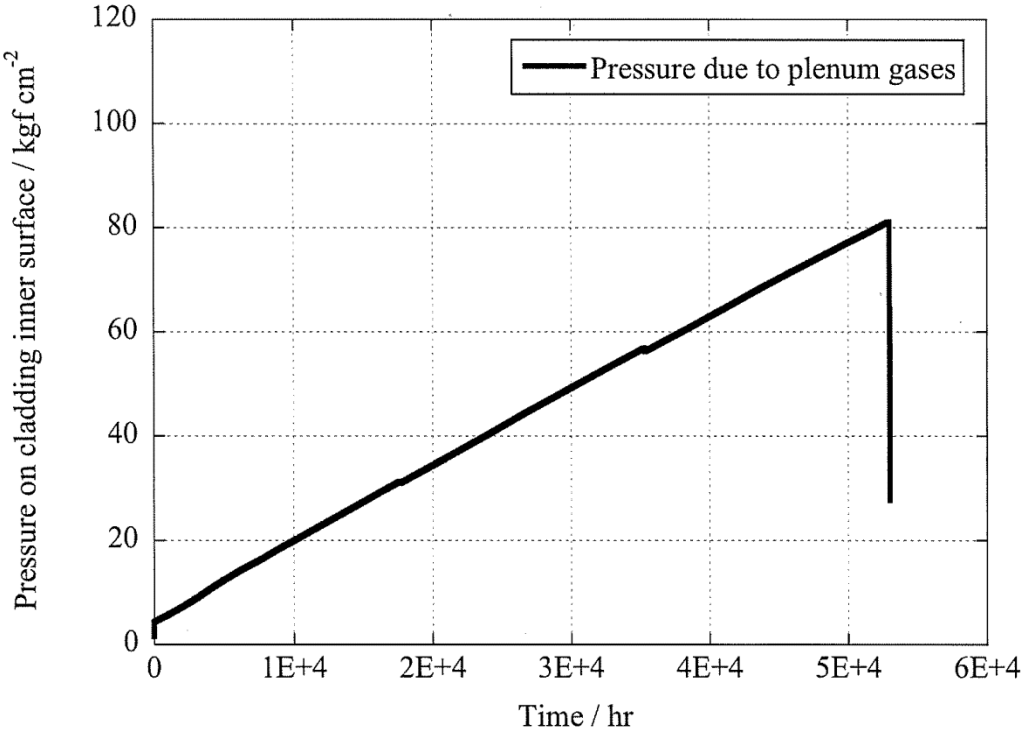

Fig.19 Profile of pressure on the cladding inner surface

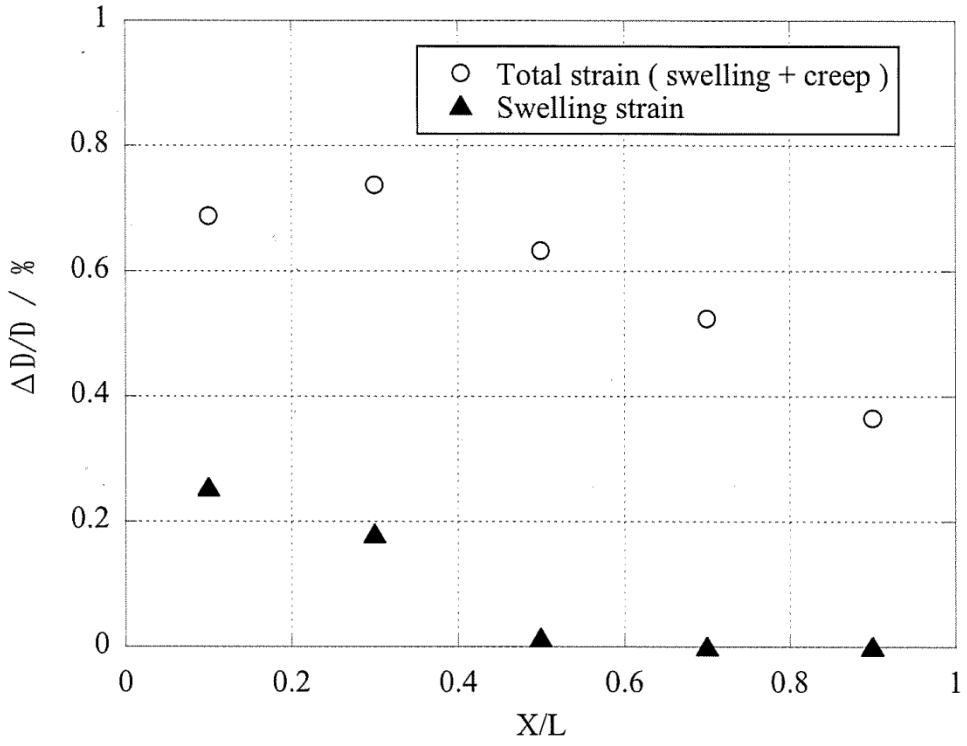

Fig.20 Cladding deformation after the irradiation

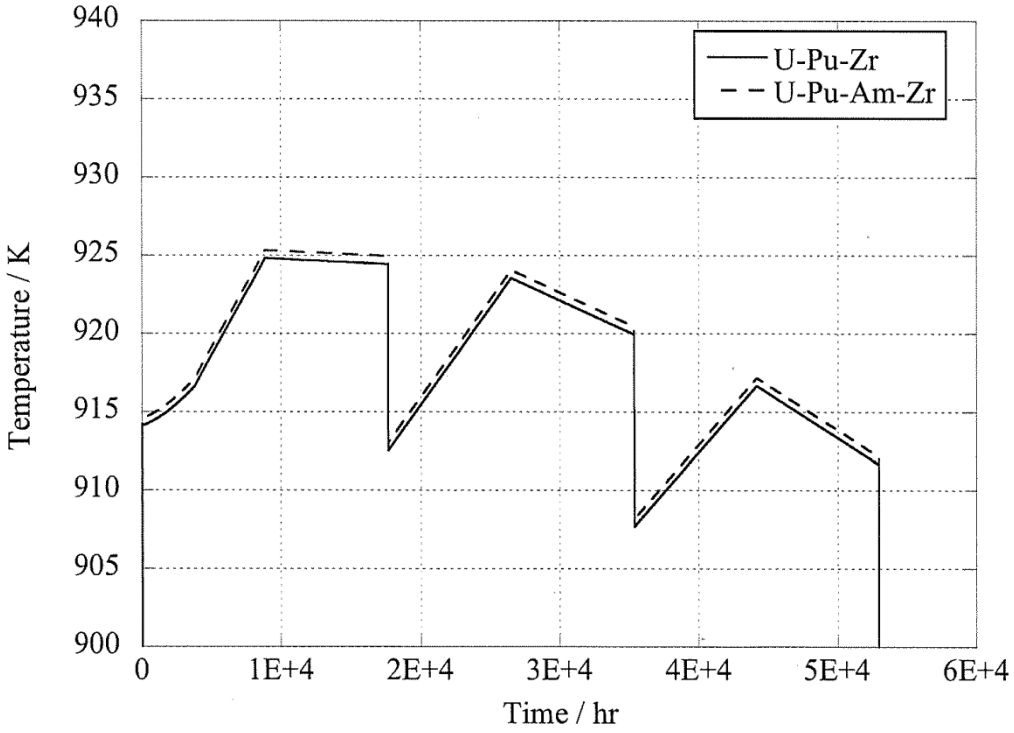

Fig.21 History of fuel center temperature at X/L=0.5
(Effective thermal conductivity model with sodium ingress into the fuel)

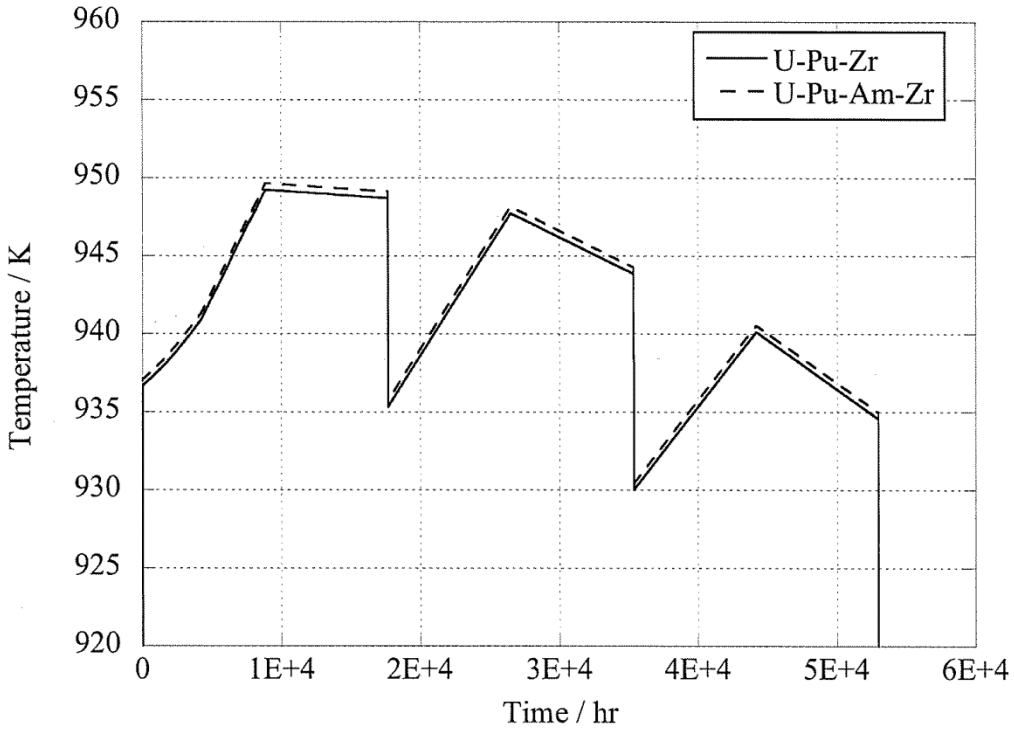

Fig.22 History of fuel center temperature at X/L=0.7
(Effective thermal conductivity model with sodium ingress into the fuel)

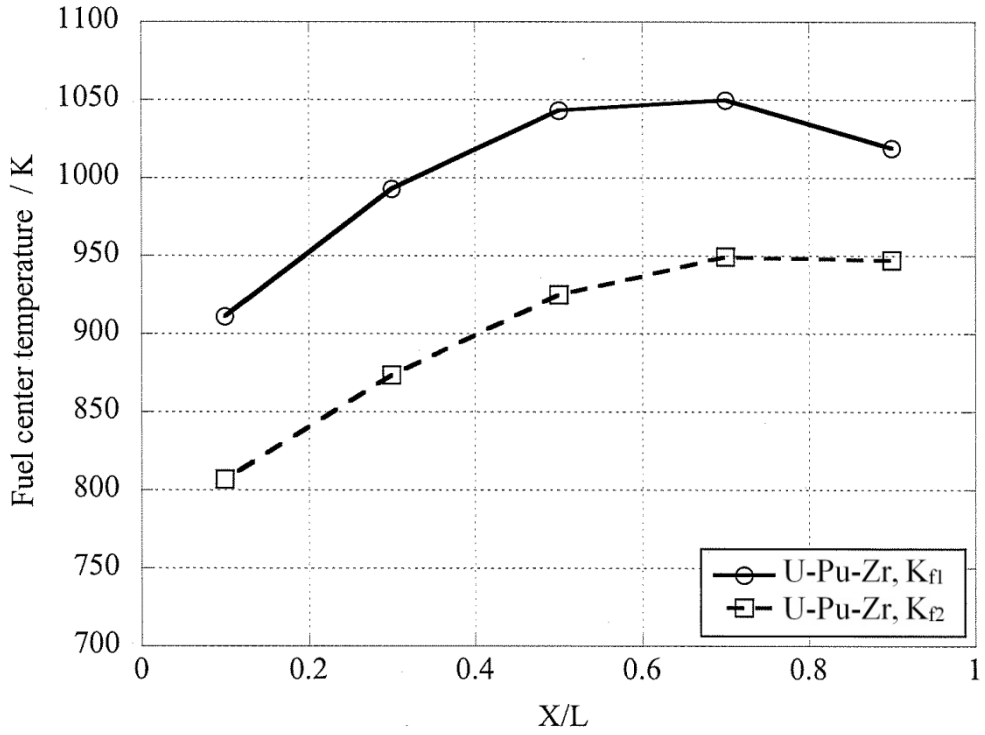

Fig.23 Axial distributions of U-Pu-Zr fuel center temperatures at the maximum power (8856h)

K_{f1} : Effective thermal conductivity model without sodium ingress into the fuel
K_{f2} : Effective thermal conductivity model with sodium ingress into the fuel

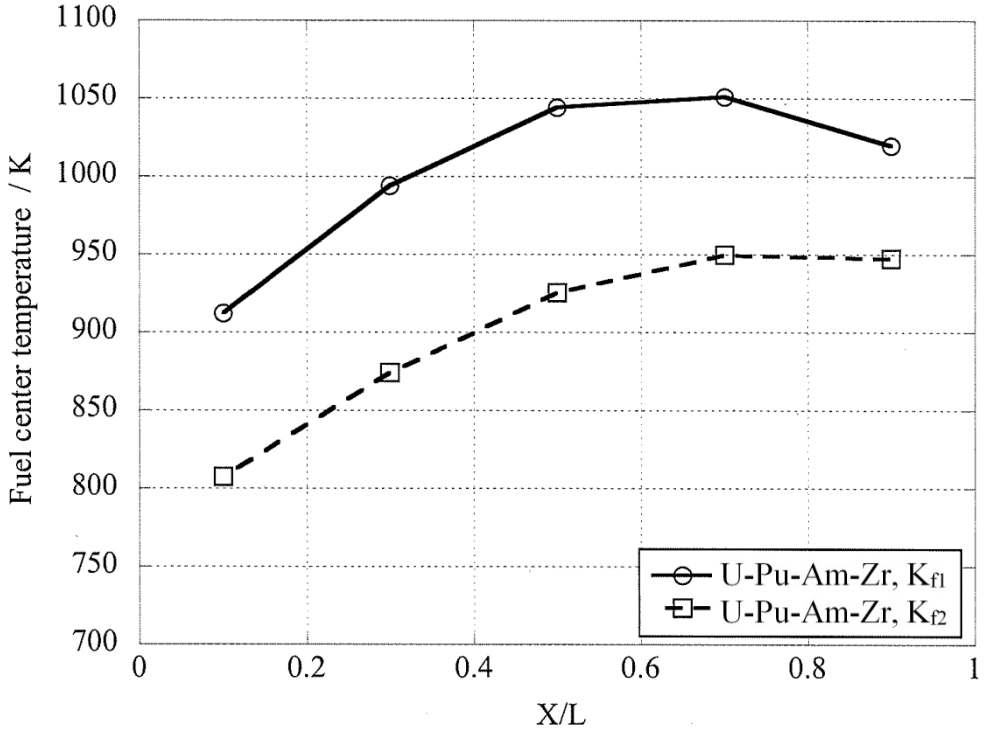

Fig.24 Axial distributions of U-Pu-Am-Zr fuel center temperatures at the maximum power (8856h)

This is a blank page.

国際単位系（SI）

表１．SI 基本単位

基本量	SI 基本単位	
	名称	記号
長さ	メートル	m
質量	キログラム	kg
時間	秒	s
電流	アンペア	A
熱力学温度	ケルビン	K
物質量	モル	mol
光度	カンデラ	cd

表２．基本単位を用いて表されるSI組立単位の例

組立量	SI 基本単位	
	名称	記号
面積	平方メートル	m^2
体積	立法メートル	m^3
速さ，速度	メートル毎秒	m/s
加速度	メートル毎秒毎秒	m/s^2
波数	毎メートル	m^{-1}
密度，質量密度	キログラム毎立方メートル	kg/m^3
面積密度	キログラム毎平方メートル	kg/m^2
比体積	立方メートル毎キログラム	m^3/kg
電流密度	アンペア毎平方メートル	A/m^2
磁界の強さ	アンペア毎メートル	A/m
量濃度(a)，濃度	モル毎立方メートル	mol/m^3
質量濃度	キログラム毎立法メートル	kg/m^3
輝度	カンデラ毎平方メートル	cd/m^2
屈折率(b)	（数字の） 1	1
比透磁率(b)	（数字の） 1	1

(a) 量濃度（amount concentration）は臨床化学の分野では物質濃度（substance concentration）ともよばれる。
(b) これらは無次元量あるいは次元１をもつ量であるが、そのことを表す単位記号である数字の１は通常は表記しない。

表３．固有の名称と記号で表されるSI組立単位

組立量	SI 組立単位			
	名称	記号	他のSI単位による表し方	SI基本単位による表し方
平面角	ラジアン(b)	rad	1 (b)	m/m
立体角	ステラジアン(b)	sr(c)	1 (b)	m^2/m^2
周波数	ヘルツ(d)	Hz		s^{-1}
力	ニュートン	N		m kg s^{-2}
圧力，応力	パスカル	Pa	N/m^2	m^{-1} kg s^{-2}
エネルギー，仕事，熱量	ジュール	J	N m	m^2 kg s^{-2}
仕事率，工率，放射束	ワット	W	J/s	m^2 kg s^{-3}
電荷，電気量	クーロン	C		s A
電位差（電圧），起電力	ボルト	V	W/A	m^2 kg s^{-3} A^{-1}
静電容量	ファラド	F	C/V	m^{-2} kg^{-1} s^4 A^2
電気抵抗	オーム	Ω	V/A	m^2 kg s^{-3} A^{-2}
コンダクタンス	ジーメンス	S	A/V	m^{-2} kg^{-1} s^3 A^2
磁束	ウエーバ	Wb	Vs	m^2 kg s^{-2} A^{-1}
磁束密度	テスラ	T	Wb/m^2	kg s^{-2} A^{-1}
インダクタンス	ヘンリー	H	Wb/A	m^2 kg s^{-2} A^{-2}
セルシウス温度	セルシウス度(e)	℃		K
光束	ルーメン	lm	cd sr(c)	cd
照度	ルクス	lx	lm/m^2	m^{-2} cd
放射性核種の放射能(f)	ベクレル(d)	Bq		s^{-1}
吸収線量，比エネルギー分与，カーマ	グレイ	Gy	J/kg	m^2 s^{-2}
線量当量，周辺線量当量，方向性線量当量，個人線量当量	シーベルト(g)	Sv	J/kg	m^2 s^{-2}
酸素活性	カタール	kat		s^{-1} mol

(a)SI接頭語は固有の名称と記号を持つ組立単位と組み合わせても使用できる。しかし接頭語を付した単位はもはやコヒーレントではない。
(b)ラジアンとステラジアンは数字の１に対する単位の特別な名称で、量についての情報をつたえるために使われる。実際には、使用する時には記号rad及びsrが用いられるが、習慣として組立単位としての記号である数字の１は明示されない。
(c)測光学ではステラジアンという名称と記号srを単位の表し方の中に、そのまま維持している。
(d)ヘルツは周期現象についてのみ、ベクレルは放射性核種の統計的過程についてのみ使用される。
(e)セルシウス度はケルビンの特別な名称で、セルシウス温度を表すために使用される。セルシウス度とケルビンの単位の大きさは同一である。したがって、温度差や温度間隔を表す数値はどちらの単位で表しても同じである。
(f)放射性核種の放射能（activity referred to a radionuclide）は、しばしば誤った用語で"radioactivity"と記される。
(g)単位シーベルト（PV,2002,70,205）についてはCIPM勧告2（CI-2002）を参照。

表４．単位の中に固有の名称と記号を含むSI組立単位の例

組立量	SI 組立単位		
	名称	記号	SI 基本単位による表し方
粘度	パスカル秒	Pa s	m^{-1} kg s^{-1}
力のモーメント	ニュートンメートル	N m	m^2 kg s^{-2}
表面張力	ニュートン毎メートル	N/m	kg s^{-2}
角速度	ラジアン毎秒	rad/s	m m^{-1} s^{-1}=s^{-1}
角加速度	ラジアン毎秒毎秒	rad/s^2	m m^{-1} s^{-2}=s^{-2}
熱流密度，放射照度	ワット毎平方メートル	W/m^2	kg s^{-3}
熱容量，エントロピー	ジュール毎ケルビン	J/K	m^2 kg s^{-2} K^{-1}
比熱容量，比エントロピー	ジュール毎キログラム毎ケルビン	J/(kg K)	m^2 s^{-2} K^{-1}
比エネルギー	ジュール毎キログラム	J/kg	m^2 s^{-2}
熱伝導率	ワット毎メートル毎ケルビン	W/(m K)	m kg s^{-3} K^{-1}
体積エネルギー	ジュール毎立方メートル	J/m^3	m^{-1} kg s^{-2}
電界の強さ	ボルト毎メートル	V/m	m kg s^{-3} A^{-1}
電荷密度	クーロン毎立方メートル	C/m^3	m^{-3} sA
表面電荷	クーロン毎平方メートル	C/m^2	m^{-2} sA
電束密度，電気変位	クーロン毎平方メートル	C/m^2	m^{-2} sA
誘電率	ファラド毎メートル	F/m	m^{-3} kg^{-1} s^4 A^2
透磁率	ヘンリー毎メートル	H/m	m kg s^{-2} A^{-2}
モルエネルギー	ジュール毎モル	J/mol	m^2 kg s^{-2} mol^{-1}
モルエントロピー，モル熱容量	ジュール毎モル毎ケルビン	J/(mol K)	m^2 kg s^{-2} K^{-1} mol^{-1}
照射線量（X線及びγ線）	クーロン毎キログラム	C/kg	kg^{-1} sA
吸収線量率	グレイ毎秒	Gy/s	m^2 s^{-3}
放射強度	ワット毎ステラジアン	W/sr	m^4 m^{-2} kg s^{-3}=m^2 kg s^{-3}
放射輝度	ワット毎平方メートル毎ステラジアン	$W/(m^2$ sr)	m^2 m^{-2} kg s^{-3}=kg s^{-3}
酵素活性濃度	カタール毎立方メートル	kat/m^3	m^{-3} s^{-1} mol

表５．SI 接頭語

乗数	接頭語	記号	乗数	接頭語	記号
10^{24}	ヨタ	Y	10^{-1}	デシ	d
10^{21}	ゼタ	Z	10^{-2}	センチ	c
10^{18}	エクサ	E	10^{-3}	ミリ	m
10^{15}	ペタ	P	10^{-6}	マイクロ	μ
10^{12}	テラ	T	10^{-9}	ナノ	n
10^9	ギガ	G	10^{-12}	ピコ	p
10^6	メガ	M	10^{-15}	フェムト	f
10^3	キロ	k	10^{-18}	アト	a
10^2	ヘクト	h	10^{-21}	ゼプト	z
10^1	デカ	da	10^{-24}	ヨクト	y

表６．SIに属さないが、SIと併用される単位

名称	記号	SI 単位による値
分	min	1 min=60s
時	h	1h =60 min=3600 s
日	d	1 d=24 h=86 400 s
度	°	1°=(π/180) rad
分	’	1’=(1/60)°=(π/10800) rad
秒	”	1”=(1/60)’=(π/648000) rad
ヘクタール	ha	$1ha=1hm^2=10^4m^2$
リットル	L, l	$1L=11=1dm^3=10^3cm^3=10^{-3}m^3$
トン	t	$1t=10^3$ kg

表７．SIに属さないが、SIと併用される単位で、SI単位で表される数値が実験的に得られるもの

名称	記号	SI 単位で表される数値
電子ボルト	eV	$1eV=1.602\ 176\ 53(14)\times10^{-19}J$
ダルトン	Da	$1Da=1.660\ 538\ 86(28)\times10^{-27}kg$
統一原子質量単位	u	1u=1 Da
天文単位	ua	$1ua=1.495\ 978\ 706\ 91(6)\times10^{11}m$

表８．SIに属さないが、SIと併用されるその他の単位

名称	記号	SI 単位で表される数値
バール	bar	$1\ bar=0.1MPa=100kPa=10^5Pa$
水銀柱ミリメートル	mmHg	1mmHg=133.322Pa
オングストローム	Å	$1\ Å=0.1nm=100pm=10^{-10}m$
海里	M	1 M=1852m
バーン	b	$1\ b=100fm^2=(10^{-12}cm)2=10^{-28}m^2$
ノット	kn	1 kn=(1852/3600)m/s
ネーパ	Np	SI単位との数値的な関係は、対数量の定義に依存。
ベル	B	
デジベル	dB	

表９．固有の名称をもつCGS組立単位

名称	記号	SI 単位で表される数値
エルグ	erg	$1\ erg=10^{-7}$ J
ダイン	dyn	$1\ dyn=10^{-5}$N
ポアズ	P	1 P=1 dyn s cm^{-2}=0.1Pa s
ストークス	St	1 St =$1cm^2$ s^{-1}=$10^{-4}m^2$ s^{-1}
スチルブ	sb	1 sb =1cd cm^{-2}=10^4cd m^{-2}
フォト	ph	1 ph=1cd sr cm^{-2} 10^4lx
ガル	Gal	1 Gal =1cm s^{-2}=$10^{-2}ms^{-2}$
マクスウェル	Mx	1 Mx = 1G cm^2=10^{-8}Wb
ガウス	G	1 G =1Mx cm^{-2} =10^{-4}T
エルステッド(c)	Oe	1 Oe ≙ $(10^3/4\pi)$A m^{-1}

(c) ３元系のCGS単位系とSIでは直接比較できないため、等号「 ≙ 」は対応関係を示すものである。

表10．SIに属さないその他の単位の例

名称	記号	SI 単位で表される数値
キュリー	Ci	$1\ Ci=3.7\times10^{10}Bq$
レントゲン	R	$1\ R=2.58\times10^{-4}C/kg$
ラド	rad	$1\ rad=1cGy=10^{-2}Gy$
レム	rem	$1\ rem=1\ cSv=10^{-2}Sv$
ガンマ	γ	1γ=1 nT=10-9T
フェルミ		1フェルミ=1 fm=10-15m
メートル系カラット		1メートル系カラット = 200 mg = 2×10-4kg
トル	Torr	1 Torr = (101 325/760) Pa
標準大気圧	atm	1 atm = 101 325 Pa
カロリー	cal	1cal=4.1858J（「15℃」カロリー），4.1868J（「IT」カロリー）4.184J（「熱化学」カロリー）
ミクロン	μ	1 μ =1μm=10^{-6}m

（第8版，2006年改訂）

この印刷物は再生紙を使用しています